

See discussions, stats, and author profiles for this publication at:
<https://www.researchgate.net/publication/244133922>

Theoretical study of thiol-induced reconstructions on the Au(1 1 1) surface

ARTICLE *in* CHEMICAL PHYSICS LETTERS · JULY 2002

Impact Factor: 1.9 · DOI: 10.1016/S0009-2614(02)00841-2

CITATIONS

141

READS

25

2 AUTHORS, INCLUDING:



Luis M Molina

Universidad de Valladolid

52 PUBLICATIONS 2,727 CITATIONS

SEE PROFILE

Theoretical study of thiol-induced reconstructions on the Au(1 1 1) surface

L.M. Molina, B. Hammer *

Interdisciplinary Nanoscience Center (iNANO), Institute of Physics and Astronomy, University of Aarhus, Ny Munkegade, Bygn. 520, DK-8000 Aarhus C, Denmark

Received 28 January 2002; in final form 15 May 2002

Abstract

A new suggestion for the structure of the Au substrate underlying self-assembled monolayers (SAM) made of thiols is presented on the basis of density functional theory results for methylthiolate ($-\text{SCH}_3$) adsorption on Au(1 1 1). It is found that by introducing vacancy defects on the substrate, the adsorption of SCH_3 is stabilized by about 0.8 eV with respect to the perfect Au(1 1 1) surface. As this overcomes the vacancy formation energy (≈ 0.6 eV), a net driving force exists leading to an adsorbate-induced reconstruction, that enhances adsorption at defected Au(1 1 1). A comparison of results at high and low SCH_3 coverage provides further insight into which specific gold vacancy sites enhance the adsorption energy of the SCH_3 molecule. © 2002 Published by Elsevier Science B.V.

In the last years, self-assembled monolayers (SAM) of organic molecules on metal surfaces have been intensely studied both for their intrinsic interest as new materials and for having potential new applications as biocompatible materials or chemical sensors [1,2]. Among them, alkanethiols on gold have attracted a great deal of interest and have become a kind of model system for SAM [3–6], due to their suitable properties for experimental work; they are easy to prepare, stable, and possess a well-defined order. One of the main issues for these systems is a precise determination of their structural features. It is commonly assumed that the thiols break the terminal S–H bond and bind

to the surface with a strong S–Au bond, while the chains interact through Van der Waals interactions. STM and LEED studies show that the SAM of alkanethiols on Au(1 1 1) may form super lattices of a $(\sqrt{3} \times \sqrt{3})R30^\circ$ structure [4,7]. However, there is some controversy about the exact location of the sulfur head groups on the surface. Besides, experimental evidence suggests that the presence of defects within the gold surface cannot be neglected; on one side, Rohwerder et al. [8] have reported the presence of mysterious holes in octadecylmercaptan SAM. On the other side, islands of Au vacancies formed after deposition of thiols have been observed [5,9]. Then, it seems that the mobility of the gold atoms in the substrate is not negligible at all. Finally, recent density functional theory (DFT) studies of $\text{SCH}_3/\text{Au}(1\ 1\ 1)$ using the slab approach show controversy about the bond

* Corresponding author: Fax: +45-8612-0740.

E-mail address: hammer@phys.au.dk (B. Hammer).

strength of sulfur to gold, indicating a too small binding to the surface compared with experiment [10–14]. As all of those simulations were performed assuming a perfectly regular Au(111) surface, there is a call for studying alternative structures.

In this Letter, we show that the $(\sqrt{3} \times \sqrt{3})R30^\circ$ supramolecular arrangement of methylthiolate on Au(111) is stabilized by a vacancy structure in the upper gold layer. The energetic cost of creating the vacancies is more than compensated by the gain in the adsorption energy of SCH₃ at the defected surface with respect to the perfect Au(111) surface case. The underlying reasons for this behaviour are associated with a higher reactivity of the defected structure, and only selected vacancy sites are particularly important for increasing the interaction energy between methylthiolate and the substrate. The Letter is outlined as follows: first, we briefly describe the theoretical approach. Second, the main results are presented for the three types of surface reconstructions under study (perfect, ‘honeycomb’ and ‘inverted-honeycomb’). Third, we analyze the detailed features of the S–Au chemical bond and its dependence on the concentration and distribution of defects on the surface. Finally, our main conclusions are presented.

The DFT calculations were performed using ultrasoft pseudopotentials [15], a plane wave basis set ($E_{\text{cut}} = 25$ Ry) and the Generalized Gradient Approximation (GGA) with the functional of Perdew and Wang (PW91) [16] for the description of exchange-correlation effects. We also report non-selfconsistent total energies obtained using the RPBE functional [17], which provides an improved description of the chemisorption energetics of CO, NO and O₂ at transition metal surfaces [17]. For the $(\sqrt{3} \times \sqrt{3})R30^\circ$ super cells, the gold substrate was simulated using a slab geometry with variable thickness: four layers of gold atoms were employed when studying the relative stabilities of the methylthiolate molecule among the different adsorption sites, whereas five layers were used for a more accurate computation of the SCH₃ adsorption potential energy at the most stable location. In both cases, two layers were kept frozen while the rest were allowed to relax. A special 18 k-points Chadi–Cohen grid [18] was used for the

simulations on a four-layers slab. For the more precise simulations on a five-layers slab, we employed a more refined grid with 54 k-points. These parameters give adsorption potential energies converged to less than 20 meV. For the (3×3) super cells, the gold substrate was simulated by three layers slab and the Brillouin zone integration was done on a 2×2 k-point grid. In order to assure that no residual strain is present in the gold substrate, the theoretical lattice parameter of solid Au (4.18 Å) was used in every case.

We start by considering the SCH₃ adsorption into the $(\sqrt{3} \times \sqrt{3})R30^\circ$ structure since this is the structure reported to be underlying experimentally observed SAMs. Given the constraints imposed by the $(\sqrt{3} \times \sqrt{3})R30^\circ$ arrangement of SCH₃ molecules on the surface, and the strong and site-selective binding of these molecules to the substrate, two defected structures are obvious candidates for stable reconstructions of the gold substrate, being the most simple possibilities: On one side, a ‘honeycomb’ (HC) structure with one gold atom missing for every three in the outermost Au layer (see Fig. 1a). On the other side, an ‘inverted-honeycomb’ (IHC) structure, with two gold atoms missing for every three. The second one can be viewed as a kind of ‘negative image’ of the first one. A number of different adsorption sites on every of the defected reconstructions under study have been considered. These are marked with black dots in Fig. 1a.

The adsorption potential energies

$$E_{\text{ads}} = E(\text{SCH}_3/\text{Au}) - E(\text{SCH}_3) - E(\text{Au}) \quad (1)$$

of the methylthiolate molecule on each of the sites for both HC and IHC reconstructed structures are shown in Table 1 (note that the energy required to form the HC or IHC reconstructions is not included). Also, for the sake of comparison, we include the adsorption potential energy on the most stable site (Bridge) for the perfect Au(111) surface. The equilibrium bending angles of the S–C bond with respect to the surface normal are also given. The bridge site (B) is the most stable location on the HC reconstruction, although the energy difference between that site and neighbouring ones is very small. Allowing full relaxation for the SCH₃ molecule, we find that a configuration for which the S head group is slightly displaced from

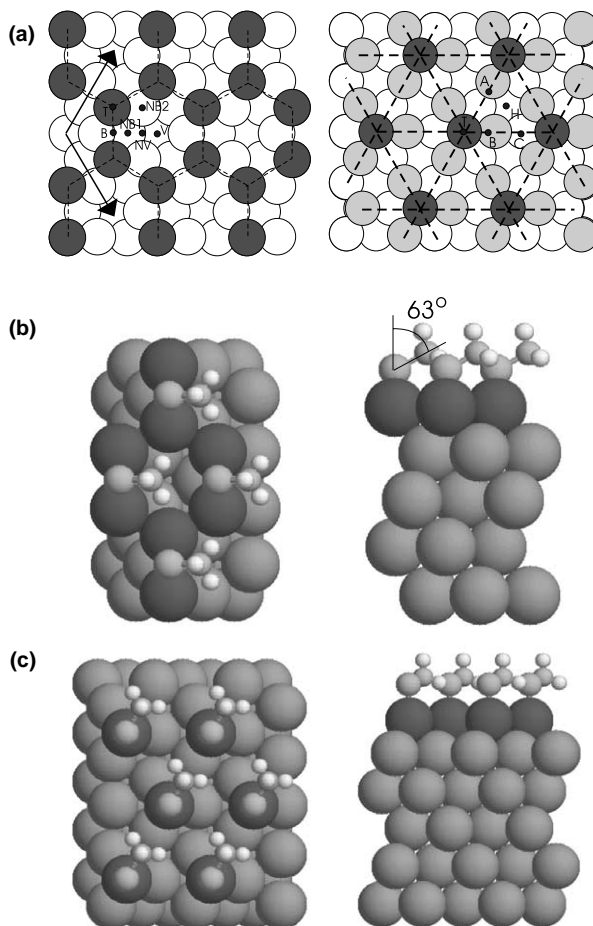


Fig. 1. (a) Top view of the HC (left) and IHC (right) reconstructions. Dark circles denote Au atoms in the outermost layer. The locations of the several adsorption sites under study are indicated by black dots. Also, the unit vectors of the $(\sqrt{3} \times \sqrt{3})R30^\circ$ unit cell are shown; (b) top (left) and side (right) views of the SCH₃ molecule adsorbed on the bridge site of the HC reconstruction; (c) the same for SCH₃ adsorbed on the top site of the IHC reconstruction.

the bridge site is energetically preferred. The structural arrangement is shown in Fig. 1b. The overall energetics, however, show that the methylthiolate sits at a very shallow potential well. It is important to stress that, excepting the vacancy site, in all cases the SCH₃ adsorbs in a bent configuration. This angle varies according to the site. It is larger for the more open sites (bridge: 63°, top: 68°) and decreases as we approach to the Au vacancy. Previous research in our group [14] for the adsorption of SCH₃ on perfect Au(111) shows that the driving force for the bending is the involvement of the sulfur 3p orbitals in the bonding, and a tendency to attain a chemical configuration

similar to that of H₂S or HSCH₃ molecules (both of them showing H–S–H and H–S–C bent angles). For the IHC reconstruction, the most stable location for methylthiolate was found to be atop of the protruding Au atom in the outermost layer (see Fig. 1c). The adsorption potential energy on the already reconstructed surface is –2.10 and –1.75 eV at the PW91 and RPBE levels, around 0.35 eV less favourable than in the case of the HC reconstruction (–2.44 and –1.94 eV), although the values are still more favorable than for the perfect surface (–1.67, –1.13 eV). This is not surprising at all, since it can be expected that more open surfaces should be more reactive and thus enhance

Table 1

Adsorption potential energies of SCH₃ on several sites of the perfect, HC and IHC reconstructions, using both PW91 and RPBE exchange-correlation functionals (in eV)

Reconst.	Site	Energy (PW91)	Energy (RPBE)	Angle
Perf.	(B)	−1.67	−1.13	58.5
HC	(V)	−1.53	−1.02	0.0
HC	(T)	−1.83	−1.43	67.9
HC	(B)	−2.44	−1.94	63.1
HC	(NB1)	−2.42	−1.96	40.2
HC	(NB2)	−2.31	−1.85	38.8
HC	(NV)	−2.16	−1.66	18.0
IHC	(T)	−2.10	−1.75	74.6
IHC	(A)	−2.00	−1.55	44.2
IHC	(B)	−1.93	−1.54	64.0
IHC	(C)	−1.89	−1.49	7.8
IHC	(H)	(A)		

The tilt angles (in degrees) between the S–C bond and the direction normal to the surface are also shown. Note that for the IHC reconstruction, the (H) site is unstable and relaxes towards the (A) site.

adsorption energies. It is interesting to note that, in the case of the HC or IHC reconstructions, the structural minimization of the surfaces prior to the adsorption of methylthiolate leads to important distortions on the interlayer equilibrium distance for the outermost Au layer. This distortion is negligible for the perfect Au(111) surface (displacements of less than a 0.5% of the interlayer distance). However, for the HC reconstruction the outermost layer is pushed down by a 6.0% of the interlayer distance. This relaxation of the outermost metallic layer can be attributed to a tendency of the undercoordinated Au atoms in that layer to get a higher electronic charge density, trying to

resemble better the perfect bulk environment [19]. For the IHC reconstruction, such reduction of the height of the first layer of gold atoms with respect to their positions in the bulk reaches 12%. Upon adsorption of SCH₃, that height is restored a little upwards, but remains to be considerably reduced (5.3% in the HC case). This could have interesting implications on detecting experimentally the adsorbate-induced reconstruction discussed below: such a noticeable departure from the coordinates of bulk Au could be observed.

The most interesting feature of the ‘honeycomb’ reconstruction is the enhanced adsorption energy of methylthiolate on it. In Table 2, we show a

Table 2

Comparison of the energetic balances for adsorption of SCH₃ (SCH₃ + Au → SCH₃/Au) and dissociative adsorption of HSCH₃ (HSCH₃ + Au → (1/2)H₂ + SCH₃/Au) on both perfect, HC and IHC Au(111) surfaces (in eV)

Reaction	PW91	RPBE	Exp.
SCH ₃ + Au(Perf.) → SCH ₃ /Au(Perf.)	−1.67	−1.13	−1.73 [2]
SCH ₃ + Au(Perf.) → SCH ₃ /Au(HC)	−1.84	−1.43	
SCH ₃ + Au(Perf.) → SCH ₃ /Au(IHC)	−1.36	−1.11	
SCH ₃ + Au(HC) → SCH ₃ /Au(HC)	−2.43	−1.93	
SCH ₃ + Au(IHC) → SCH ₃ /Au(IHC)	−2.07	−1.70	
HSCH ₃ + Au(Perf.) → (1/2)H ₂ + SCH ₃ /Au(Perf.)	−0.11	+0.32	−0.22 [2]
HSCH ₃ + Au(Perf.) → (1/2)H ₂ + SCH ₃ /Au(HC)	−0.29	+0.03	
HSCH ₃ + Au(Perf.) → (1/2)H ₂ + SCH ₃ /Au(IHC)	+0.06	+0.26	
HSCH ₃ + Au(HC) → (1/2)H ₂ + SCH ₃ /Au(HC)	−0.88	−0.47	
HSCH ₃ + Au(IHC) → (1/2)H ₂ + SCH ₃ /Au(IHC)	−0.65	−0.33	

PW91, RPBE and experimental results are given.

comparison between the energies of the $\text{SCH}_3 + \text{Au} \rightarrow \text{SCH}_3/\text{Au}$ and $\text{HSCH}_3 + \text{Au} \rightarrow (1/2)\text{H}_2 + \text{SCH}_3/\text{Au}$ reactions, for both perfect, HC and IHC gold surfaces. It must be stressed that here we report results obtained using the more accurate 5-layers and 54 \mathbf{k} -points approach (therefore, some quantities are slightly different in Tables 1 and 2). Besides, the energy required to form the reconstructed HC and IHC surfaces is included for some of the reactions. The adsorption potential energy of SCH_3 on $\text{Au}(111)$ is stabilized by around 0.8 eV on going from the perfect (−1.67 eV at the PW91 level) to the HC structure (−2.43 eV). Consequently, the energetic balance of the dissociative adsorption of HSCH_3 on $\text{Au}(111)$ is changed by the same amount, from −0.11 to −0.88 eV (PW91). Of course, on simulating the formation of a SCH_3 monolayer over the defected gold surface it must be taken into account that it costs some energy to create the Au vacancies. Such vacancy formation energy has been calculated with the same first principles approach as

$$E_{\text{defect}} = E(\text{Au}_{\text{reconstructed}}) + n \cdot E(\text{Au}_{\text{bulk}}) - E(\text{Au}_{\text{perfect}}), \quad (2)$$

being $E(\text{Au}_{\text{perfect}})$ the energy of the unreconstructed $\text{Au}(111)$ surface, $E(\text{Au}_{\text{reconstructed}})$ the energy of the reconstructed one, $E(\text{Au}_{\text{bulk}})$ the energy per atom in bulk Au, and n the number of vacancies created per unit cell (1 for HC, 2 for IHC). For the HC surface, it amounts to 0.59 eV using the PW91 functional and 0.50 eV with the RPBE one. Then, by adding this energy cost to the adsorption potential energies, we can obtain overall PW91/RPBE reaction energies of −1.84/−1.43 eV for thiolate + $\text{Au}(\text{Perfect}) \rightarrow \text{thiolate}/\text{Au}(\text{HC})$ and −0.29/+0.03 eV for thiol + $\text{Au}(\text{Perfect}) \rightarrow (1/2)\text{H}_2 + \text{thiolate}/\text{Au}(\text{HC})$. These values compare much better with experiments (−0.22 eV [2]) than the ones obtained assuming a perfect (111) gold surface. Clearly, there is a driving force that favours the formation of the HC structure, as there is a net stabilization of approximately 0.2 eV with respect to the perfect $\text{Au}(111)$ surface. Consequently, our results seriously suggest the possibility of an adsorbate-induced reconstruction on forming SAMs made of thiols. On the contrary, the IHC reconstruction is clearly not favoured.

The energy gained upon adsorption with respect to the perfect $\text{Au}(111)$ case (around 0.4 eV) does not compensate, as in the HC case, the cost for creating the reconstruction, that amounts to 0.71 and 0.59 eV per Au atom at the PW91 and RPBE levels, respectively. Consequently, the energetic balance of the dissociative adsorption reaction for this reconstruction results in positive values. Finally, we will mention that, although the RPBE values do not provide a better agreement with experiment than the PW91 ones, we include them for completeness and for showing that the adsorbate-induced reconstruction effect observed is quite insensitive to the exchange-correlation functional employed.

In Fig. 2, we plot a contour map of the adsorption induced electronic charge density difference

$$\rho_{\text{induced}} = \rho(\text{SCH}_3/\text{Au}) - \rho(\text{Au}) - \rho(\text{SCH}_3) \quad (3)$$

for the SCH_3 molecule adsorbed in the bridge site of the HC reconstruction. $\rho(\text{SCH}_3/\text{Au})$, $\rho(\text{Au})$ and $\rho(\text{SCH}_3)$ denote the charge densities of the

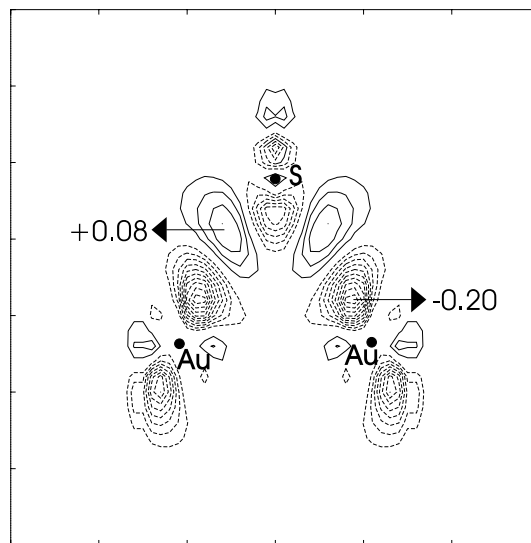


Fig. 2. Contour map of the valence charge density difference ρ_{induced} in the vertical plane formed by the sulfur atom in methylthiolate adsorbed in the bridge site of the HC reconstruction and its two Au nearest neighbours. The position of those atoms is indicated in the plot. Positive and negative differences are represented by solid and dashed contours, respectively. The arrows mark the values of the minimum and maximum charge density differences (in $\text{e}^-/\text{\AA}^3$). Step size between contours: $0.02 \text{ e}^-/\text{\AA}^3$.

whole SCH_3/Au system, the clean defective $\text{Au}(111)$ surface and the free (but strained) SCH_3 molecule, respectively. The induced charge density is plotted in a vertical plane containing the sulfur atom and the two gold atoms with which the sulfur coordinates. The adsorption induced charge density provides interesting information about the nature of the bonding between the sulfur head group and the substrate. The main contribution to the bond arises from hybridization between the sulfur $3p_z$ orbitals and the d_z^2 orbitals of the two Au atoms nearest to the sulfur. There is a depletion of charge (minus signs) on these orbitals, and an accumulation in regions halfway between the sulfur and gold atoms. Consequently, the bonding has an important covalent character.

A comparative analysis of the bonding features for both perfect and defective (honeycomb) substrates was carried out, showing remarkably similar features in both cases. Induced charge densities and projections of the density of states into sulfur and gold orbitals were compared for both situations, giving no sizable differences able to provide a clear chemical explanation for the 0.8 eV energy gain in the adsorption energy of methylthiolate when vacancies are included. The results suggest that the most likely reason for a preference of the HC reconstruction must be a special stabilization of the Au–Au bonds in the honeycomb structure upon adsorption of SCH_3 (with respect to the perfect $\text{Au}(111)$ case), rather than an enhancement of the bond strength between sulfur and its two nearest neighbours due to the presence of nearby vacancies. In order to shed light to the role of neighbouring vacancies on enhancing SCH_3 binding, additional calculations at much smaller SCH_3 coverage $\theta = 1/9$ (realized in the larger $p(3 \times 3)$ unit cell) were performed. The purpose of this was to isolate the interaction between vacancy defects, in order to clarify which precise vacancy sites do change the SCH_3 binding to the substrate. Fig. 3 shows a view of the unit cell for the perfect $\text{Au}(111)$ surface, with labels for each of sites surrounding the two Au atoms where SCH_3 sits ('B' sites). In Fig. 4a the adsorption energies of methylthiolate (hollow symbols) on a number of different reconstructions are presented, as a function of the number of vacancies per unit cell. Each data is labelled with

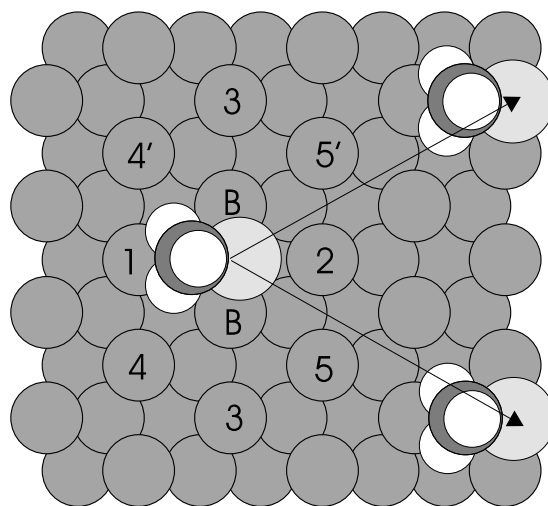


Fig. 3. View of the SCH_3 molecule adsorbed on a perfect $\text{Au}(111)$ surface, with a $c(3 \times 3)$ unit cell. Different sites are labelled: B represent the two Au atoms to which SCH_3 is chemically bond, and sites 1–5 denote all the inequivalent nearest neighbours of the B atoms. Arrows mark the unit cell vectors.

numbers indicating which atoms were removed when creating the vacancies (note that because of the shape of the unit cell employed, both atoms labelled '3' are the same, so removing it creates vacancies both above and below of each of the B sites). Also, the energetic cost for the formation of the defected reconstructions is shown (filled squares). The figure shows a steady increase of the reactivity at the B sites as the number of vacancies increases (or as the coordination of the 'B' atoms decrease). This is not at all surprising, since it is generally known that the intrinsic reactivity of noble atoms rises as coordination decreases [20–22]. A striking result seen in the figure is that only vacancies 1 and 2 enhance significantly the adsorption energy of SCH_3 , and no major changes are obtained on removing atoms at the other neighbouring sites. Besides, as the energy gain obtained by removing either atom 1 or atom 2 is roughly the same, an explanation of higher SCH_3 binding energy in terms of less steric repulsion between the CH_3 group and atom 1 in the HC phase can be clearly ruled out. For the $p(3 \times 3)$ unit cell with low SCH_3 coverage, the cost of forming any vacancy structure is greater than the gain in the SCH_3 adsorption energy. This is unlike the situation at high coverage

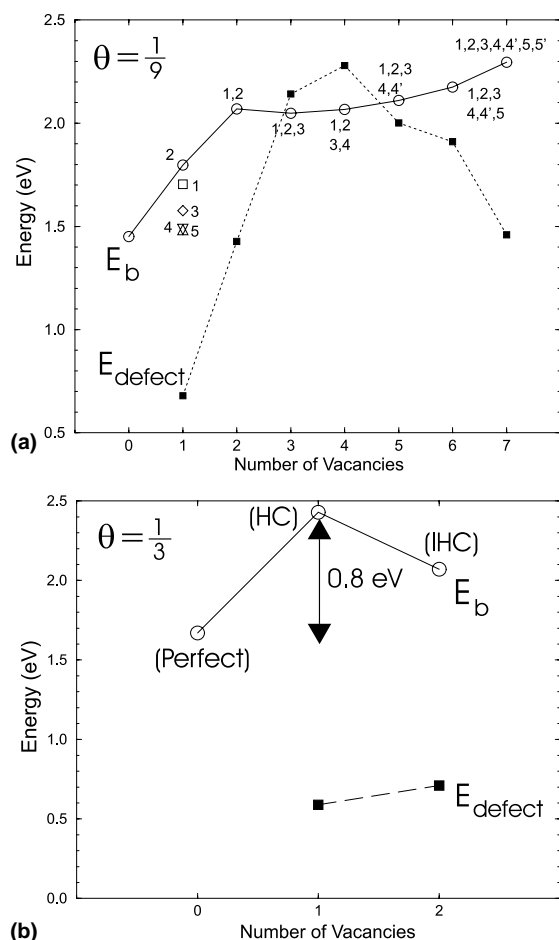


Fig. 4. (a) Adsorption energy E_b (= minus the adsorption potential energy) of methylthiolate (hollow symbols) as a function of the number of vacancies in a $c(3 \times 3)$ unit cell ($1/9$ coverage). Numbers indicate the sites removed on creating the different defected surfaces (see text and Fig. 3). Black squares indicate the energy required to create the defected surfaces (E_{defect}); (b) results for a $(\sqrt{3} \times \sqrt{3})R30^\circ$ unit cell ($1/3$ coverage) with perfect, HC and IHC surfaces (0, 1 and 2 vacancies per cell, respectively).

($\theta = 1/3$), already discussed for the $(\sqrt{3} \times \sqrt{3})R30^\circ$ structure. For completeness Fig. 4b presents the vacancy formation energies and SCH_3 adsorption energies for this coverage, showing that the energetics is optimized by the adsorption induced vacancy formation.

A number of interesting consequences come out once it has been checked the important influence of vacancies present at both sides of the bridge site.

The most remarkable one is that the honeycomb reconstruction, together with a $(\sqrt{3} \times \sqrt{3})R30^\circ$ arrangement of the SCH_3 molecules on the surface, is the only way of having vacancies at both sides of each methylthiolate molecule adsorbed in the surface, with a *minimum* number of vacancies (and consequently minimal energetic cost for creating a defected surface) per methylthiolate unit. However, as the net energy gain (once discounted the vacancy formation energy) on including vacancies is not very large (with respect to the perfect surface case), still alternative proposals involving mixed situations with a lower concentration of vacancies are possible. This gives a hint why a $c(4 \times 2)$ super structure phase has been observed experimentally [23–25]. This phase is characterized by a unit cell containing four methylthiolate molecules divided in two groups of two equivalent ones. Then, models including up to four vacancies per unit cell (that corresponds to a HC arrangement), either with similar, or with varying orientations of the SCH_3 units, and with a preference for vacancy locations at one or both sides of the bridge sites seem feasible and likely to explain the experimental data. During the writing of this manuscript, we learned that Morikawa et al. [26] completely independently from us have already taken some steps in this direction, confirming the existence of a net driving force towards adsorbate-induced vacancy formation.

Finally, concerning a possible influence of the thiol chain length on the ability of the thiol molecules to induce surface reconstruction, we are confident that such ability would be unchanged for longer chains. This effect is mainly due to the local chemical interaction of the sulfur head group with the surface, so changes of the type of thiol would probably only affect the detailed features of the SAM at a much larger scale (maybe having influence on the type of network formed by the Au vacancies). These considerations are also supported by recent calculations by Morikawa et al. [27] showing that both binding strength and bonding geometry do not change on passing from methylthiolate to ethylthiolate or butylthiolate.

In conclusion, in this Letter we have shown that density functional theory provides strong support for a possible adsorbate-induced reconstruction of the Au(111) surface during the ad-

sorption of thiol molecules. Evidence for this arises mainly from a better agreement with experimental data for the energetics of the dissociative adsorption of HSCH₃ on Au(111), when a defective honeycomb-like gold surface is considered. The driving force for that is the higher binding energy of SCH₃ on such defective reconstruction. It is crucial that the extra energy gained during the adsorption of methylthiolate more than compensates the cost of creating the Au vacancies on the surface.

Acknowledgements

Discussions with A. Kuhnle, T.R. Linderöth and F. Besenbacher are gratefully acknowledged. This work was supported by The Danish Research Councils.

References

- [1] F. Schreiber, *Prog. Surf. Sci.* 65 (2000) 151.
- [2] A. Ulman, *Chem. Rev.* 96 (1996) 1533.
- [3] G.E. Poirier, E.D. Pylant, *Science* 272 (1996) 1145.
- [4] L.H. Doboïs, B.R. Zegarski, R.G. Nuzzo, *J. Chem. Phys.* 98 (1993) 678.
- [5] G.E. Poirier, *Chem. Rev.* 97 (1997) 1117.
- [6] H. Kondoh, C. Kodama, H. Sumida, H. Nozoye, *J. Chem. Phys.* 111 (1999) 1175.
- [7] N. Camillone III, C.E.D. Chidsey, G. Liu, G. Scoles, *J. Chem. Phys.* 98 (1993) 3503.
- [8] M. Rohwerder, K. Deweldige, E. Vago, H. Viefhaus, M. Stratmann, *Thin Solid Films* 264 (1995) 240.
- [9] K. Edinger, A. Götzhäuser, K. Demota, Ch. Wöll, M. Grunze, *Langmuir* 9 (1993) 4.
- [10] H. Grönbeck, A. Curioni, W. Andreoni, *J. Am. Chem. Soc.* 122 (2000) 3839.
- [11] Y. Yourdshahyan, H.K. Zhang, A.M. Rappe, *Phys. Rev. B* 63 (2001) 081405.
- [12] T. Hayashi, Y. Morikawa, H. Nozoye, *J. Chem. Phys.* 114 (2001) 7615.
- [13] M.C. Vargas, P. Giannozzi, A. Selloni, G. Scoles, *J. Phys. Chem.* 105 (2001) 9509.
- [14] J. Gottschalk, B. Hammer, *J. Chem. Phys.* 116 (2002) 784.
- [15] D.H. Vanderbilt, *Phys. Rev. B* 41 (1990) 7892.
- [16] J.P. Perdew, J.A. Chevary, S.H. Vosko, K.A. Jackson, M.R. Pederson, D.J. Singh, C. Fiolhais, *Phys. Rev. B* 46 (1992) 6671.
- [17] B. Hammer, L.B. Hansen, J.K. Nørskov, *Phys. Rev. B* 59 (1999) 7413.
- [18] D.J. Chadi, M.L. Cohen, *Phys. Rev. B* 8 (1973) 5747.
- [19] K.W. Jacobsen, J.K. Nørskov, M.J. Puska, *Phys. Rev. B* 35 (1987) 7423.
- [20] E. Shustorovich, *Adv. Catal.* 37 (1990) 101.
- [21] E. Hansen, M. Neurock, *Surf. Sci.* 441 (1999) 410.
- [22] B. Hammer, J.K. Nørskov, *Adv. Catal.* 45 (2000) 71.
- [23] N. Camillone, C.E.D. Chidsey, G.-Y. Liu, G. Scoles, *J. Chem. Phys.* 98 (1993) 4234.
- [24] P. Fenter, P. Eisenberger, K.S. Liang, *Phys. Rev. Lett.* 70 (1993) 2447.
- [25] G.E. Poirier, M.J. Tarlov, *Langmuir* 10 (1994) 2853.
- [26] Y. Morikawa, C.C. Liew, H. Nozoye, *Surf. Sci.* (submitted).
- [27] Y. Morikawa, T. Hayashi, C.C. Liew, H. Nozoye, *Surf. Sci.* (in press).